# Proton-Proton Collisions at 4.2 Bev*

M. H. Blue†, J. J. Lord, J. G. Parks, and C. H. Tsao
*Department of Physics, University of Washington, Seattle, Washington*
(Received March 27, 1961; revised manuscript received October 5, 1961)

Interactions between 4.15-Bev protons and the free hydrogen nuclei in nuclear emulsion are examined. The total elastic cross section from 27 events was determined to be 11.0±2.6 mb. On the basis of 113 interactions the total inelastic cross section was found to be 28.1±3.1 mb. The partial cross sections corresponding to inelastic collisions having two, four, six, and eight secondary particles were found to be respectively 16.3±2.4, 11.5±1.8, 0.2±0.1, and 0.1±0.1 mb. While the total inelastic cross section varies slowly with energy, the partial inelastic cross sections were found to be strongly energy dependent. The observed angular distribution of elastically scattered protons in the center-of-mass system was sharply peaked in the forward and backward directions, in fair agreement with calculations based on a simple optical model applicable for energies between 2 and 10 Bev. Particles produced in inelastic collisions were identified as pions or protons by measurements of energy loss and multiple scattering. For those particles identified, center-of-mass system distributions of energy, angle, and transverse momentum are presented.

## I. INTRODUCTION

THE study in detail of the proton-proton interaction at energy ranges from 1 to 30 Bev allows the examination of some salient features of this interaction. Certain features such as the multiplicity of pion production are very strongly energy dependent in this energy region. The angular distribution of particles produced in the interaction, their energy distribution, and the elastic scattering process are all important in the consideration of this problem. The influence of nucleonic isobars, pion-pion final state interaction, and considerations of single boson exchanges all deserve attention. While in many cases the experimental results are considerably in advance of their interpretation, it is anticipated that more detailed knowledge of the processes observed will aid in understanding the high-energy proton-proton interaction.

This paper reports the results of an investigation of the scattering of 4.2-Bev kinetic energy protons by free hydrogen nuclei in nuclear emulsion. Data are presented for the elastic scattering angular distribution and the absolute cross section for elastic scattering as well as for cross sections of inelastic processes producing events with two, four, and six or more charged secondary particles. About two thirds of the particles produced in inelastic interactions are identified as being pions or protons as a result of ionization and multiple scattering measurements. Data are also presented on the center-of-mass system distributions of the kinetic energy, and scattering angle for the identified charged secondary particles produced in inelastic events. In addition, data are presented on the $Q$ values calculated for these cases where pion-pion and pion-proton particle pairs were identified.

* Work supported by the National Science Foundation, and by the joint program of the U. S. Atomic Energy Commission and the Office of Naval Research.

† Present address: Lawrence Radiation Laboratory, Livermore, California.

## II. PROCEDURE

### A. Exposure and Scanning

In this experiment a stack of 36 four-inch square by 600-$\mu$ thick Ilford G-5 pellicles was exposed to a 4.15 ±0.05 Bev interval beam of the Berkeley Bevatron for a cumulative stack exposure of about $10^7$ protons. The pellicle orientation during the exposure was such that incident particles entered the stack edge and then traveled nearly parallel to the plane of the emulsion. After the emulsions were mounted on glass and developed using standard techniques it was found that this exposure resulted in a flux which was approximately a Gaussian function of $y$, the distance from one edge of the emulsion parallel to the beam direction. The measured flux values were about $5\times10^5$ and $8\times10^4$ beam protons/cm$^2$ at $y$ values of 1 cm and 4 cm, respectively.

The plates were then scanned for proton-proton like interactions by the method of following secondary particles as described by Kalbach *et al.*[1] The interactions located in scanning were subsequently re-examined and any nuclear interaction which could not be a proton-proton collision was called a star. Those interactions selected as proton-proton-like collisions had to meet the following criteria:

(1) An event must have an even number of prongs (secondary tracks).

(2) An event must have no recoil blob or decay electron, evidence of being a collision with a proton bound in the nucleus of a heavier element of the emulsion.

(3) An event can have neither alpha-particle tracks, nor more than one slow proton, nor any protons with a laboratory scattering angle greater than 90°.

Criterion (1) arises from consideration of the reactions

$$\begin{aligned} p+p &\rightarrow p+p+(a\pi^+ + a\pi^-)+b\pi^0 \\ &\rightarrow p+n+\pi^+ + (a\pi^+ + a\pi^-)+b\pi^0 \\ &\rightarrow n+n+\pi^+ + R^+ + (a\pi^+ + a\pi^-)+b\pi^0, \end{aligned}$$

[1] R. M. Kalbach, J. J. Lord, and C. H. Tsao, Phys. Rev. **113**, 325 and 330 (1959).

for which $a+2b$ can only take values consistent with the production of 10 or fewer mesons at the energy of this experiment. We have by inspection the conclusion that proton-proton collisons must have an even number By similar reasoning applied to the case of the neutron target reactions

$$\begin{aligned} p+n &\rightarrow p+p+\pi^-+a(\pi^++\pi^-)+b\pi^0 \\ &\rightarrow p+n \quad\quad +a(\pi^++\pi^-)+b\pi^0 \\ &\rightarrow n+n+\pi^++a(\pi^++\pi^-)+b\pi^0, \end{aligned}$$

we conclude that all odd-pronged events must be associated with proton-proton collisions. However, this even-odd classification scheme will be reversed for events in which one of the secondary particles undergoes a charge exchange reaction with a neighboring nucleon. We have considered the effect this pheonmenon would have to our cross-section determinations and found it both small and partially compensated by similar reactions of the particles from proton-neutron interactions. Criteria (2) and (3) above are working standards used to eliminate some of the events located as being collisions with bound protons.

## B. Measurement of Events

### *1. Elastic Proton-Proton Collisions*

The angular measurements to be described were made on all of the two prong events which appeared to be approximately coplanar and which had observed scattering angles approximately consistent with the kinematics of elastic scattering.

All microscopes were equipped with a cross-hair disk in one ocular which, when used in connection with an attached angular scale, allowed one to measure the projected angle between two tracks to within 0.5°. Dip angles were ascertained by measuring the change in depth of a track together with the corresponding projected track length. This change in depth was measured by taking advantage of the limited depth of field at large magnifications and a calibrated scale attached to the fine focusing adjustment of the microscope. Dip angles for most tracks were measured to within 0.5°. The space angles of the secondary protons, and the degree of coplanarity of the three proton tracks were determined from the measured dip and projected angles by plotting these data on a 40-cm diameter stereographic projection calibrated in 1° intervals. Two-prong events were then accepted as being elastic collisions with free hydrogen nuclei if the combined kinematic and coplanar errors were less than 1.5°.[1]

### *2. Inelastic Events*

In addition to the angular measurements described above, grain density and multiple scattering or range measurements were made on most inelastic secondaries. With the aid of the theoretical dependence of the rate of energy loss on momentum times velocity,[2] such data were combined to determine the mass and momentum of the secondaries. In instances where a secondary particle comes to rest in the emulsion, measurement of its range and examination of the track ending is sufficient to establish its identity and energy. When the secondary particle did not stop in the emulsion its track was subjected to grain desnity and multiple scattering measurements. The grain density (closely related to the energy loss) of a track was expressed in terms of $g$, the ratio of the grain count (grains/100 $\mu$) of the track to that of a beam proton track passing through the emulsion at the same average depth. Multiple scattering measurements were carried out with several different cell lengths and the data treated in terms of second differences.[1]

The relation between the mean absolute second difference due to multiple scattering $\langle D_m \rangle$, the momentum $p$, and the velocity $v$, is

$$pv=(K_z Z L^{\frac{2}{3}})/(573\langle D_m \rangle). \quad (1)$$

In Eq. (1), $K_z$ is the scattering factor, $Z$ is the atomic number of the moving particle, and $L$ is the cell length in microns. When $\langle D_m \rangle$ is in microns, $pv$ is in Mev. For this experiment, the value of $K_z$ was taken to be 25, a value consistent with available data for G-5 emulsions.[3]

The experimental second differences, $\langle D_e \rangle$, are subject to systematic errors due to differential shrinkage of the emulsions during processing, spurious scattering, and noise in the scattering stage and associated measuring apparatus. The commonly occurring type of differential shrinkage which will distort an originally straight track into a C-shaped curve can be taken into account by considering third differences.[4] However, in this experiment, a slightly different procedure was adopted for corrections to the observed second differences, $\langle D_e \rangle$. On the assumption that the emulsion C-shaped distortion over a limited region of the plate will transform a straight track into one which is a sector of a circle, a corrected second difference $\langle D_e \rangle$ was calculated. The expected contributions to the observed second differences due to apparatus noise and spurious scattering were evaluated by performing multiple scattering measurements with various cell lengths on a Bausch and Lomb straight line, and on the primary 4.2-Bev proton tracks. Since the spurious scattering average second differences, $\langle D_{ss} \rangle$, are approximately proportional to the cell length[5] and the average noise second difference, $\langle D_n \rangle$, are independent of cell length, it is possible to separate and evaluate these effects. Assuming Gaussian

[2] R. M. Sternheimer, Phys. Rev. **88**, 851 (1952); **91**, 256 (1952).
[3] C. Fichtel and M. W. Friedlander, Nuovo cimento **10**, 1032 (1958).
[4] S. Biswas, B. Peters, and H. Rama, Proc. Indian Acad. Sci. **A41**, 154 (1955).
[5] F. W. Fischer and J. J. Lord, Nuovo cimento **11**, 44 (1959).

distributions of second differences it follows that[5]

$$\langle D_e' \rangle^2 \simeq \langle D_m \rangle^2 + \langle D_{ss} \rangle^2 + \langle D_n \rangle^2. \quad (2)$$

The mean second differences $\langle D_m \rangle$ obtained from the observed multiple scattering and the above corrections were used in Eq. (1) to obtain $pv$ for the secondary particles.

A theoretical relation[2] between $g$ and $pv$ was then used to identify the secondary particles as being pions or protons. $K$ mesons were not considered because of the relatively low production cross section and the experimental difficulty in distinguishing between protons and $K$ mesons. An IBM 650 computer was used to perform the calculations necessary to obtain particle identities and momenta using the observed data ($g$, $pv$, and their standard deviations) and the relations between these quantities. If the ionization loss vs $pv$ curves for both pions and protons were plotted, this computation would be equivalent to ascertaining the proper (most probable) curve with which the data ($g$, $pv$, and their standard deviations) should be associated and the point on this proper curve which represents the most probable value of $pv$ for the secondary particle under consideration. In some cases where the identification was not obvious, the momentum and scattering angle were examined under both pion and proton assumptions. The correct choice was sometimes more obvious when such values were considered in the light of scattering angles and momentum values for the remaining secondaries of a particular event, while in some cases this procedure led to the rejection of an event because of an obvious momentum unbalance for either assumption. In the present work we were able to identify all of the charged particles in a given event for only a small number of cases. Accordingly, this discussion of momentum balancing pertains only to the identified charged particles we examined. This is also the reason for carrying out the analysis by classifying events according to the number of secondary tracks rather than according to a scheme requiring knowledge of neutral secondary particles.

Some tracks are so steep in the emulsion as to render data of their multiple scattering inconclusive. In addition as noted by others,[1,6] the combined results of multiple scattering and blob count data may lie in a region of the $g$ vs $pv$ plot[2] which is awkward for purposes of particle identification. However, a considerable number (about two-thirds) of the secondary tracks involved in this study were classed as identifiable and are the basis of the results reported herein.

With a knowledge of the scattering angle, identity, and momentum of a particular secondary, the scattering angle, energy, and momentum in the center-of-mass system, subsequently referred to as the c.m.-system, were determined using standard transformation equations.

### C. Cross-Section Determinations

In order to calculate cross sections and other relevant information on the proton-proton interaction at 4.2 Bev it is necessary to make corrections for scanning and other biases in this experiment. The corrections are made easier, as noted by Kalbach *et al.*,[1] since the scanning efficiency for tracks having dip angles (angle with the plane of the emulsion) $\beta \leq 10°$ depends only on the plane-projected angle $\phi$ between the track under consideration and the direction of the beam protons.

In order to make scanning efficiency corrections, two distributions of tracks with respect to $\phi$ were constructed; one for tracks followed to stars in the course of the original scan and another for the set of scanner acceptable-type tracks[7] from a sample of stars located by area scanning. (Fig. 3 of reference 1). Then a differential scanning efficiency[1] function $\epsilon(\phi)$ was defined as the ratio of the ordinates of these distributions evaluated at a given angle $\phi$. If $n(\phi)$ represents the normalized number of tracks followed to stars, then the total scanning efficiency is given by $\epsilon_t = \int n(\phi)\epsilon(\phi)d\phi$. Finally, if $N'$ is the total number of events of a given type which were found, then the number corrected for scanning efficiency is $N = N'/\epsilon_t$. In Table I, $N'$ is given in the second row and $N$ is the third row.

A correction also was made for the mean multiplicity of scanner acceptable tracks per event. This correction takes into account the fact that events of high multiplicity of charge secondary particles are more readily found than those of lower multiplicity. For example, elastic collisions at these energies are characterized by having only a single track in the forward direction and the correction for multiplicity in this case is unity as shown in row 4 of Table I. For the other classes of events in row 4, the multiplicity correction was taken to be the ratio of the total number of events located to the total number of scanner acceptable tracks.

It is evident that the criteria used in selecting events for this experiment are not adequate to eliminate all edge-on (quasi-free) collisions of beam protons with nuclei other than protons. However, it was concluded that at a bombarding energy of 4.2 Bev, the Fermi momentum of such bound protons would not materially effect the energy spectra or angular distributions of secondary pions and protons. On the other hand, for a determination of cross sections, it is necessary to know the fraction of events satisfying the criteria listed above in Sec. II.A, which are actually collisions with heavy nuclei.

---

[6] R. R. Daniel, N. Kameswara Rao, P. K. Malhotra, and Y. Tsuzuki, Nuovo cimento **16**, 1 (1960).

[7] A scanner acceptable track is defined as one having a relative grain dens ty $g \leq 1.4$ t mes minimum ionization and a dip angle $\beta \leq 10°$, which is consistent with the criteria originally used by the scanners in selecting tracks to follow.

TABLE I. Events found in scanning and applied corrections.

| Event type (prong number) | Elastic 2 | Inelastic events 2 | 4 | 6 | 8 | Stars |
|---|---|---|---|---|---|---|
| Number found in scanning, $N'$ | 27 | 58 | 56 | 4 | 1 | 648 |
| Number corrected for scanning efficiency, $N$ | 32.0 | 93.1 | 81.3 | 2.5 | 1.3 | 1042 |
| Number corrected for multiplicity | 32.0 | 67.5 | 42.3 | 0.6 | 0.3 | 1681 |
| Number corrected for quasi-free collisions (output number of events), $\mathfrak{N}$ | 26.3 | 37.1 | 26.2 | 0.4 | 0.2 | 1681 |
| Resulting cross section in millibarns | 11.6 | 16.3 | 11.5 | 0.2 | 0.1 | |

For elastic collisions it is well known[1,8,9] that this separation of events into "good" and "bad" can be made with some confidence. The method, also used in this work, consists of making precise measurements of the scattering angles and only accepting events which, to within the measurement errors, are coplanar and have scattering angles consistent with the kinematics of elastic scattering. From a frequency distribution of the composite angluar deviation from exact coplanarity and elastic kinematics (Fig. 2 of reference 1) the number of quasi-free events is readily determined. This correction amounted to about 20% as is shown in row 5 of Table I.

For inelastic events, determination of the fraction $F$ of these events which are interactions with heavy nuclei is more complicated. We used average values of this fraction for elastic events from the present work in combination with $F$(elastic) from the data of Kalbach, Cester, and Duke to ascertain $F$(2-prong inelastic) and then used Kalbach's determination of the prong dependence of $F$ for events of higher multiplicity. The final corrected data are shown in row 5 of Table I. The fact that our resulting total and elastic cross sections agree to those obtained by other workers in the same energy region (Fig. 2) lends confidence to this procedure.

The mean free path for the collision of 4.2-Bev protons with emulsion nuclei was found by "along the track scanning."[10] In this experiment the mean free path for star production was found to be $\lambda_s=40.2$ cm, in agreement with that found by other observers[8–12] at Bev energies.

Using a hydrogen content for nuclear emulsion of $(3.34\pm0.1)\times10^{22}$ nuclei per cubic centimeter,[13] the partial cross section for a given type of event is $\sigma_x=297\mathfrak{N}_x/\lambda_s\mathfrak{N}_s$ mb, where $\mathfrak{N}_x$, as shown in row 5 of Table I, is the corrected number of events of a certain class $\mathfrak{N}_s$ is the corrected number of stars. The calculated cross sections in this experiment are given in row 6 of Table I.

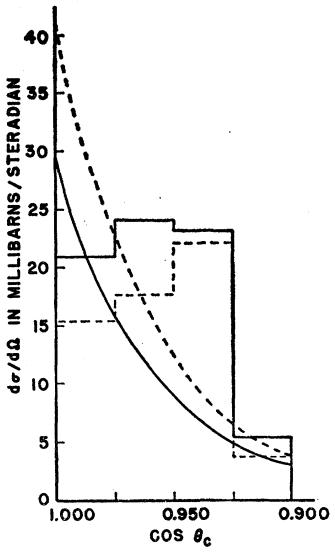


FIG. 1. Center-of-mass system angular distribution of elastically scattered protons. The dashed histogram represents the observed distribution, while the solid histrogram gives the distribution after corrections have been applied. The dashed curve is the angular distribution calculated from a disk-type optical model with radius $R=0.91$ fermi and a passing wave amplitude $a=0.316$. The solid curve is from the same type model with $R=0.94$ f and $a=0.453$.

## III. RESULTS

### A. Elastic Scattering

The angular distribution of the elastically scattered protons is shown by the solid histogram in Fig. 1. There the cross section per sterradian is plotted as a function of the cosine of the scattering angle in the center-of-mass system. The dashed histogram represents the original experimental data, while the results of correcting these data for scanning efficiency and quasi-elastic collisions are shown in the solid histogram. The elastic collision total cross secton as shown in Table I was calculated to be $11.6\pm2.6$ mb based on 27 cases of scattering.

An analysis of these data was carried out through the optical model approach. Calculations were made for both a uniform spherical and a disk model.[14] The dashed curve in Fig. 1 is a calculation based on a purely absorbing disk with a radius $R=0.91$ fermi and a passing wave amplitude of $a=0.32$. These parameters were selected from summaries given by Kalbach *et al.*[1] and Grishin *et al.*[15] They give fair agreement with experimental data for elastic scattering from 2 to 10 Bev.

A homogeneous spherical optical model with $R=1.00$ f and $a=0.32$ and the model used by Cork and coworkers[16] to fit their data at 4.4 Bev were also compared

[8] W. O. Lock, P. V. March, H. Muirhead, and W. G. V. Rosser, Proc. Roy. Soc. (London) **A230**, 215 (1955).
[9] L. W. Smith, C. P. Leavitt, A. M. Shapiro, C. E. Swartz, and M. Widgoff, Phys. Rev. **92**, 851 (1953).
[10] R. E. Cavanaugh, D. M. Haskin, and M. Schein, Phys. Rev. **100**, 1263 (1955).
[11] V. Y. Rajopadhye, Phil. Mag. **5**, 537 (1960).
[12] H. Winzeler, B. Klaiber, W. Koch, M. Nikolic, and M. Schneeberger, Nuovo cimento **17**, 8 (1960).
[13] Private communication from C. Waller, Ilford Ltd.
[14] S. Fernbach, R. Serber, and T. B. Taylor, Phys. Rev. **75**, 1352 (1949).
[15] V. G. Grishin, I. S. Saitov, and I. V. Chuvilo, Soviet Phys.—JETP **7**, 844 (1958).
[16] B. Cork, W. Wenzel, and C. Causey, Phys. Rev. **107**, 859 (1957).

TABLE II. Partial cross sections as a function of prong number.

| Number of secondary prongs | Cross section, mb |
|---|---|
| 2 (elastic) | 11.6±2.6 |
| 2 (inelastic) | 16.3±2.4 |
| 4 | 11.5±1.8 |
| 6 | 0.2±0.1 |
| 8 | 0.1±0.1 |
| All events | 39.7±4.0 |
| All inelastic events | 28.1±3.1 |

to the experimental results of Fig. 1. For both of these cases the calculated angluar distribution curves overlapped the dashed curve of Fig. 1 to such an extent that they were not included in this drawing.

The elastic proton-proton scattering measurements of Markov *et al.*[17] at 8.5 Bev includes a good deal of analysis based on small angles of scattering. Here the best fit to the data with a purely absorbing disk was obtained with $R=0.94$ and $a=0.453$. When these parameters are used for 4.15-Bev protons the solid curve in Fig. 1 is obtained.

The work of Markov *et al.*[17] also indicated that there is a possible interference between the Coulomb and nuclear diffraction scattering. Their experimental results were interpreted as showing a destructive interference which resulted in a suppression of scattering at angles less than $I_c=2°$. While the scanning techniques used in the present experiment provided a number of small-angle scatterings in the laboratory system, the smallest plane-projected angle we observed was 1.1° with our detection efficiency noticeably approaching zero for projected angles less than 2.0°. (3.9° and 7.2° in the c.m.-system). However, the plane of this 1.1° projected-angle event was tilted with respect to the emulsion plane, corresponding to a spatial-scattering angle of 2.8° (10.0° in the c.m.-system). Accordingly, while the results of the present experiment (Fig. 1) suggest confirmation of this Coulomb-nuclear interference effect, the angular limitations discussed above as well as our limited statistics do not allow any definitive conclusions to be reached.

TABLE III. Energy dependence of inelastic processes.

| Proton energy (Bev) | Partial cross sections in mb 2 prongs | 4 prongs | 6 prongs | 8 prongs |
|---|---|---|---|---|
| 6.15[a] | 7.3 | 12.1 | 2.7 | 0.3 |
| 4.15[b] | 16.3 | 11.5 | 0.2 | 0.1 |
| 2.75[c] | 21.8 | 4.2 | ... | ... |
| 1.50[d] | 25.9 | 1.1 | ... | ... |

[a] See reference 1.
[b] Present work.
[c] M. M. Block, E. M. Harth, V. T. Cocconi, E. Hart, W. B. Fowler, R. P. Shutt, A. M. Thorndike, and W. L. Whittemore, Phys. Rev. **103**, 1484 (1956).
[d] W. B. Fowler, R. P. Shutt, A. M. Thorndike, and W. L. Whittemore, Phys. Rev. **103**, 1479 (1956).

[17] P. K. Markov, E. N. Tayganov, M. G. Schafranova, and B. A. Shakhbasyan, Soviet Phys.—JETP **38**, 1471 (1960).

## B. Inelastic Collisions

### *1. Cross Sections*

The partial cross sections as determined in Sec. II.C of this paper are summarized in Table II. The errors shown in Table II were obtained by considering the uncertainties in all of the correction factors discussed in Sec. II.C as well as the statistical errors due to the numbers of events. The partial cross sections are given for inelastic collisions having 2, 4, 6, and 8 charged secondary particles (prongs). The total inelastic cross section in this experiment was found to be 28.1±3.1 mb, based on 113 collisions found.

The elastic, inelastic, and total cross sections for proton-proton scattering obtained in this experiment appear in Fig. 2 together with the results of other experiments.[17–23] Tentative curves have been drawn in the figure for these three cross sections. It appears that the total cross section slowly decreases with increasing energy from 1 Bev and levels off at about 40 mb above 10 Bev. On the other hand the inelastic cross section

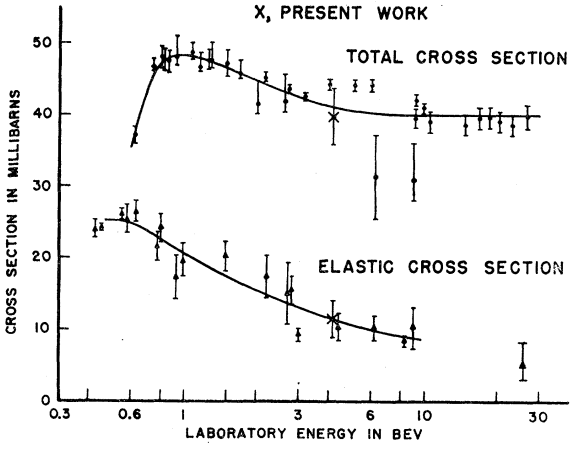


FIG. 2. A summary of proton-proton cross-section measurements in the Bev range. The upper set of points represent observations of the total cross section and the lower triangle points are for elastic scattering. The dashed curve shows the inelastic cross section. Data are taken from references 1, 11, 12, 15–23.

[18] R. Chester, T. F. Hoag, and A. Kernan, Phys. Rev. **103**, 1143 (1956).
[19] N. P. Bogachev, S. A. Bunyatov, Yu. P. Merekov, and V. M. Sikorov, Doklady Akad. Nauk. S.S.S.R. **121**, 617 (1958).
[20] M. J. Longo, J. A. Holland, W. N. Hess, B. J. Moyer, and V. Perez-Mendez, Phys. Rev. Letters **3**, 568 (1959).
[21] G. von Dardel, D. H. Frisch, R. Mermod, R. H. Milburn, P. A. Piroué, M. Vivargent, G. Weber, and K. Winter, Phys. Rev. Letters **5**, 333 (1960).
[22] H. Ashmore, G. Cocconi, A. N. Diddens, and A. M. Wetherell, Phys. Rev. Letters **5**, 576 (1960).
[23] G. Cvijanovich, B. Dayton, P. Egli, B. Klaiber, W. Koch, M. Nikolic, R. Schneeberger, H. Winzeler, J. C. Combe, W. M. Gibson, W. O. Lock, M. Scheeberger, and G. Vanderhaeghe, Nuovo cimento **20**, 1012 (1961).

remains nearly constant at 30 mb from 1 Bev to the highest measured energy of 10 Bev. The behavior of the elastic cross section from 1 to 10 Bev is similar to that for the total cross section due to the constancy of the inelastic cross section in this energy interval.

About two-thirds of the particles emitted in the inelastic collisions could be identified as protons or pions. From the numbers of particles identified and the partial cross sections shown in Table II it was possible to calculate the average multiplicity of charged pions produced in a collision. When considering all collisions the average multiplicity was found to be $1.43\pm0.3$, or if only inelastic collisions are considered, the multiplicity is $2.02\pm0.4$.

The partial cross sections observed in this experiment are compared in Table III with those at energies of 1.5, 2.75, and 6.2 Bev. As seen in Table III, there is a striking dependence of the partial cross sections upon energy. For instance the partial cross section for 4-prong events increases by a factor of 12 while the energy available in the center-of-mass system increases by only a factor of 3. In the same energy range the partial cross section for two prong events decreases by a factor of 3.5. Within statistical errors, the partial cross sections in Table III were found to be linear functions of the c.m. system energy.

### 2. *Energy and Angular Distribution of Emitted Particles*

As described above, the identity and energy of about two thirds of the emitted particles were measured. The energy spectrum of the protons from inelastic collisions is shown by the solid histogram in Fig. 3. The dashed histogram on the figure represents the energy spectrum due to protons from two-prong events. Since two-prong inelastic events represent those having lower multiplicity of pion production, it follows that, within statistical errors, there is not much dependence of the proton energy spectrum on the multiplicity of pion production.

The proton energy spectrum in Fig. 3 is similar in shape to that calculated by Cerulus *et al.*[24,25] at 2.75 Bev and 6.2 Bev. However, the experimental value of the most probable energy is slightly lower than that given by most statistical theories, even when nucleon isobars and pion-pion interactions are considered.[24,25]

The energy spectrum of the emitted charged pions is given in Fig. 4. It is to be noticed that the average center-of-mass system energy of the pions, 146 Mev, is much less than that for the protons, 305 Mev. Again the shape of the spectrum is similar to that given by Cerulus *et al.*[24 25] but the experimental value of the most probable pion energy is very much less than that given by the statistical theory.

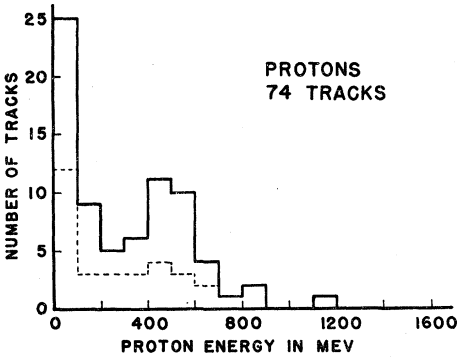


FIG. 3. Center-of-mass system energy distribution of the protons from inelastic events. The solid line is for all protons and the dashed line is for protons from 2-prong events.

There has been considerable interest in the transverse momentum of the particules emitted in high energy nucleon-nucleon collisions. An analysis of the present experiment presented elsewhere[26] showed that the pions and protons produced in inelastic interactions have a strong maximum at about 90 Mev/$c$ and 180 Mev/$c$, respectively. The arithmetic mean transverse momentum for pions was found to be 142 Mev/$c$, and that for the protons was 265 Mev/$c$.

The angular distributions of the emitted particles were determined for both protons and pions; the observations are presented in the form of the histograms shown in Figs. 5 and 6. In each histogram the number of tracks is plotted as a function of the cosine of the scattering angle in the center-of-mass system. The distributions were made symmetric in the center-of-mass system by combining the respective distributions in the forward and backward hemispheres. In this experiment, as in the observations of Kalbach *et al.*[1], the asymmetries were about the order of magnitude of those expected from statistical fluctuations; however, it is to be expected that some of this asymmetry is due to quasi-free

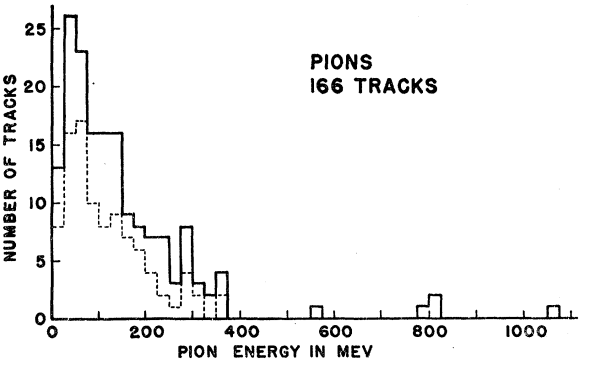


FIG. 4. Center-of-mass system energy distribution of the pions from inelastic events. The solid line is for all pions and the dashed line is for pions from 4-prong events.

[24] F. Cerulus and J. von Behr, Nuovo cimento **16**, 1046 (1960).
[25] F. Cerulus and R. Hagedorn, CERN Report 59-3, 1959 (unpublished).

[26] M. H. Blue, J. J. Lord, J. G. Parks, and C. H. Tsao, Nuovo cimento **20**, 274 (1961).

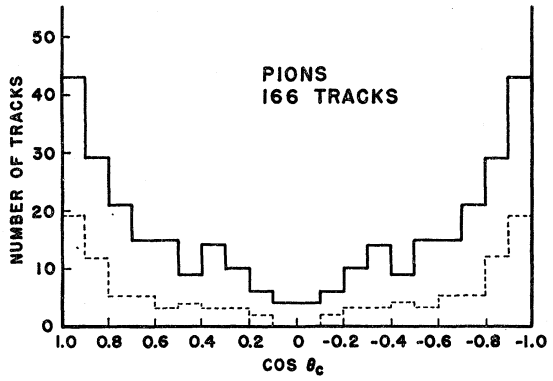


FIG. 5. Center-of-mass system angular distribution of the pions produced in inelastic events. The solid histogram is for all pions, while the dashed one is for pions from 2-prong events.

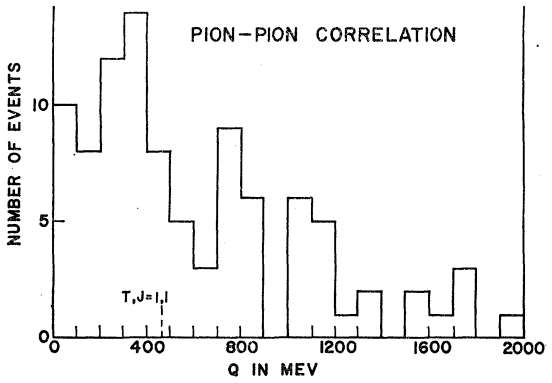


FIG. 7. Pion-pion $Q$ values for all pairs of identified charged pions in a single event.

proton-proton collisions which account for about 42% of the collisions used in this part of the experiment.

The pion angular distribution, Fig. 5, is characterized by a strong probability for pions to be emitted in the forward and backward directions. Similar angular distributions have been observed at nearby energies.[1,7,12,13,27] It was of interest as well to consider events of higher multiplicity. The pion angular distribution for events of 6 and 8 prongs was found to be isotropic in the c.m. system within experimental statistics based on 12 tracks. This effect has been noted before[1,23] and is suggestive that these events represent central collisions.

The angular distribution of all pions in Fig. 5 is evidence for the approach taken by Cerulus *et al.*[24,25] and Salzman[28] in which single pion exchange interactions are of importance in the proton-proton interaction at Bev energies. Support for this view is given also by the even stronger forward-backward angular distribution of the secondary protons as shown in Fig. 6.

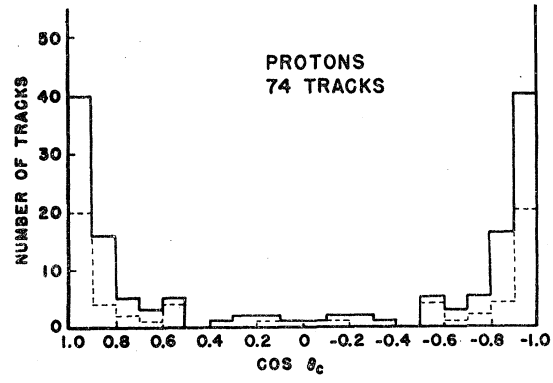


FIG. 6. Center-of-mass system angular distribution of the protons from inelastic events. The solid histogram is for all protons while the dashed one is for protons from 2-prong events.

A separate analysis for particle correlations was carried out for the two thirds of the emitted pions or protons which could both be identified and their energies determined with a precision better than 20%. For each event, the $Q$ values were calculated for all possible pairs. These data were grouped and presented in the form of the histograms shown in Figs. 7 and 8. In Fig. 7, the distribution of $Q$ values is shown for charged pion pairs. As can be seen, most of the $Q$ values lie below 500 Mev with just a slight indication of a peak between 300 and 400 Mev. It has been noted by Pickup *et al.*[29] that for certain pairs of pions ($\pi^+-\pi^-$) there is a striking maximum in the $Q$ distribution near 350 Mev.

When correlations between pions and protons were examined in terms of their $Q$ values, the histogram shown in Fig. 8 was obtained. It is important to compare this histogram of $Q$'s with the $Q$ values corresponding to the resonances observed from pion-proton scattering. At the present time resonances in the pion-proton system have been observed which yield $Q$ values of 150 Mev, 430 Mev, 600 Mev, and possibly one at 850 Mev. The histogram in Fig. 8 gives rough evidence for contributions of these isobaric states. Of course, on

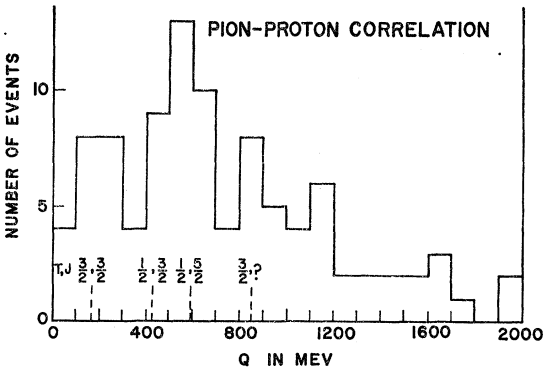


FIG. 8. Pion-proton $Q$ values.

[27] W. B. Fowler, R. P. Shutt, A. M. Thorndike, W. L. Whittemore, V. T. Cocconi, E. Hart, M. M. Block, E. M. Harth, E. C. Fowler, J. D. Garrison, and T. W. Morris, Phys. Rev. **103**, 1489 (1956).

[28] F. Salzman and G. Salzman, Phys. Rev. Letters **5**, 377 (1960).

[29] E. Pickup, F. Ayer, and E. O. Salant, Phys. Rev. Letters **5**, 611 (1960).

the basis of measuring errors, the $Q$ distributions for the 430-Mev and 600-Mev states would be expected to overlap.

Since the $Q$ distribution in Fig. 8 appears to be influenced so greatly by the pion-proton isobars, perhaps as much as 50% of the pion production in this experiment took place through isobaric-nucleon states. Sternheimer and Lindenbaum[30] have considered the influence of these isobaric nucleon states upon proton-proton interactions for energies as high as 3 Bev. Their calculations for pion production tend to shift the energy spectrum of emitted pions towards lower energies than the pure statistical theory. However, the energy spectrum of pions shown in Fig. 4 is much lower than can be accounted for by the isobaric model.

Modifications of the original statistical theory of pion production and consideration of peripheral interactions have tended to give a better interpretation of many aspects of the proton-proton interaction at energies of several Bev. However, in this experiment and others between 3 and 25 Bev there are several important features of the proton-proton interaction for which there is no really satisfactory account: (a) the large forward-backward asymmetry in the angular distribution of emitted pions in the c.m. system, (b) the tendency for most pions to be produced at low energies in the c.m. system, and (c) the large fraction of the total cross section which is in the form of elastic scattering.

[30] R. M. Sternheimer and S. J. Lindenbaum, Phys. Rev. **123**, 333 (1961).

## ACKNOWLEDGMENTS

We are indebted to Professors John S. Blair, E. M. Henley, S. Kaneko, Y. B. Kim, G. E. Masek, S. H. Neddermeyer, and R. W. Williams for many helpful discussions. Assistance in scanning the plates was provided by Miss Joyce Mumby, Miss Karen Wier, Mr. C. Y. Kim, and Mr. Frank Yen. The able assistance of Mr. P. M. Ogden in making multiple scattering measurements is gratefully acknowledged. Mr. J. A. Kirk was generally helpful during the course of this work. Dr. R. M. Kalbach was very informative and helpful during the early phases of the investigation. The exposure was arranged through the courtesy of Dr. E. J. Lofgren, Dr. W. Chupp, Dr. Harry Heard, and the Bevatron staff.